Differing Phenotypes between Intraepithelial and Stromal Lymphocytes in Early-Stage Tongue Cancer

Fuminori Katou,[1] Haruo Ohtani,[2] Yoshiko Watanabe,[1] Takashi Nakayama,[3] Osamu Yoshie,[3] and Kenji Hashimoto[1]

[1]Department of Oral and Maxillofacial Surgery, Hamamatsu University School of Medicine, Hamamatsu, Japan; [2]Department of Pathology, Mito Medical Center, National Hospital Organization, Ibaraki, Japan; and [3]Department of Microbiology, Kinki University School of Medicine, Osaka, Japan

Abstract

The significance of tumor-infiltrating lymphocytes (TIL) has attracted much attention in relation to the prognosis of patients. We herein examined the activation status of the TILs in relation to the tumor microenvironment. By using frozen sections of human early-stage tongue cancers (n = 22), the TILs in the cancer nests and those in the cancer stroma were compared for the expression of PD-1, NKG2A, NKG2D, CD69, and Ki-67. The lymphocytes in oral lichen planus, an active immune response-mediated mucosal disease, were also analyzed for comparison purposes. All of the cancer specimens were abundantly infiltrated by $CD8^+$ T cells and $CD56^+$ natural killer (NK) cells in the stroma, as well as in the tumor nest. The tumor nest–infiltrating (intraepithelial) $CD8^+$ T cells frequently expressed PD-1, an inhibitory receptor, in sharp contrast to those in the stroma or in the lichen planus. Conversely, the intraepithelial $CD8^+$ T cells only infrequently expressed NKG2D, an activating receptor, in contrast to those in the stroma or in the lichen planus. No intraepithelial $CD8^+$ T cells expressed Ki-67, a proliferation-associated marker, whereas those in the stroma frequently expressed it. Furthermore, the intraepithelial NK cells expressed NKG2A, an inhibitory receptor, more frequently than those in the stroma or the lichen planus. Collectively, the intraepithelial $CD8^+$ T cells and NK cells are phenotypically inactivated, whereas stromal counterparts are phenotypically just as active as those in the lichen planus. These results suggest the first-step occurrence of an immune evasion mechanism in the tumor nest of oral squamous cell carcinoma. [Cancer Res 2007;67(23):11195–201]

Introduction

The clinicopathologic significance of the tumor-infiltrating lymphocytes (TIL) in various human cancers has been an issue of great interest. $CD8^+$ cytotoxic T cells (CTL) and natural killer (NK) cells are the most likely effector cells for an effective antitumor immunity (1). Previous studies have shown that the infiltration of lymphocytes significantly correlates with a prolonged survival time of patients, at least in certain types of cancer (2–4). However, the capacity of the TILs as effector cells may be affected by the microenvironmental milieu of the tumor tissue (5). It could therefore be important to assess the functional state of the TILs in relation to their localization in the tumor tissue.

The functional state of the TILs may be presumed by the expression of CD69, PD-1, NKG2D, and NKG2A on $CD8^+$ T cells and NK cells for the following reasons. The CTLs express CD69 upon an acute activation with T-cell receptor engagement (6), and the NK cells also express it during the earliest activation (7, 8). PD-1 is expressed by activated T cells, and the engagement of PD-1 by PD-L1 (B7-H1), the ligand of PD-1, leads to the inhibition of the T-cell receptor–mediated T cell proliferation and cytokine secretion (9). The expression of PD-1 by CTLs thus predicts their functional exhaustion (10). NK cells are closely regulated by a balance between the signals transmitted by activating receptors (NKG2D) that recognize the ligands on tumors and by inhibitory receptors (NKG2A) that recognize HLA-E to protect HLA class I transfectants from NK cell–mediated lysis (11, 12). The engagement of NKG2A with its ligand prevents NK cell activation (13, 14). $CD8^+$ T cells and NK cells expressing NKG2D exert cytolytic responses against tumor cells expressing MICA, a ligand for NKG2D (15, 16).

In the present study, we immunophenotypically compared the TILs within the cancer nests (intraepithelial TILs) and those in the stroma near the invasion front of cancer (stromal TILs) using early-stage tongue cancers, most of which are abundantly infiltrated by the TILs. We also examined infiltrating lymphocytes in tissue specimens of oral lichen planus (OLP), which is characterized by a band-like infiltration of $CD4^+$ and $CD8^+$ lymphocytes in the submucosa, a disruption of the basement membrane, and a degeneration of the basal keratinocytes. We considered this lesion as a good positive control of an active immune-cell attack (17, 18). We herein show that the intraepithelial $CD8^+$ T cells and NK cells are predominantly of the immunosuppressed phenotypes, whereas their stromal counterparts displayed more activated phenotypes. We will discuss the significance of such different phenotypes in the TILs in view of the immune evasion by the tumor cells.

Materials and Methods

Tissue specimens. We collected tissue samples of the early-stage tongue cancer (T1-T2 N0) through biopsies or through surgical procedures during 2003 and 2006 at Hamamatsu University Hospital (n = 22). None of the patients received preoperative chemotherapy or irradiation therapy. The biopsy specimens of OLP were obtained from the buccal lesions in the exacerbation phase of disease (n = 7). The biopsies of OLP were performed before the initiation of topical or systemic therapy. The biopsies from the normal lingual mucosa of healthy volunteers (n = 4) were used as controls for immunohistochemistry. This study was approved by the Ethical Committee of Hamamatsu University School of Medicine. For quantitative real-time PCR, samples were snap-frozen and stored at −80°C. For enzyme-linked immunohistochemistry, the specimens were fixed in

Note: Supplementary data for this article are available at Cancer Research Online (http://cancerres.aacrjournals.org/).

Requests for reprints: Fuminori Katou, Department of Oral and Maxillofacial Surgery, Hamamatsu University School of Medicine, 1-20-1 Handayama, Higashi-ward, Hamamatsu 431-3125, Japan. Phone: 81-53-435-2349; Fax: 81-53-435-2349; E-mail: Katou@hama-med.ac.jp.

doi:10.1158/0008-5472.CAN-07-2637

periodate-lysine–4% paraformaldehyde (4% PLP) overnight at 4°C. After washing in PBS-containing sucrose, the fixed specimens were embedded in OCT compound (Miles), and they were then immediately frozen. For the immunofluorescent method (we only used the double labeling method), snap-frozen specimens were used in six cases.

Antibodies and immunohistochemistry. We used commercially available antibodies for the immunoperoxidase staining using fixed frozen sections in all cases (for details, see Supplementary data).

Double immunostaining. We performed double-labeling immunofluorescent microscopy in six representative cases for a more accurate cellular identification using fresh frozen specimens and enzyme-linked double immunohistochemistry in all 22 cases using PLP-prefixed specimens for quantitative analyses as described previously (for details, see Supplementary data; refs. 19, 20).

Quantitative real-time PCR. Total RNA was prepared from normal tongue tissues ($n = 2$), early squamous cell carcinoma ($n = 2$), and OLP ($n = 2$) by using Trizol reagent (Life Technologies-Bethesda Research Laboratories). Total RNA was further purified by using RNeasy (Qiagen). Total RNA (1 μg) was reverse transcribed using an oligo$(dT)_{18}$ primer and SuperScript II transcriptase (Life Technologies-Bethesda Research Laboratories). The quantitative real-time PCR was performed using the Taqman assay and 7900 HT fast real-time PCR system (Applied Biosystems). The conditions for PCR were 50°C for 2 min, 95°C for 10 min, and then 50 cycles of 95°C for 15 s (denaturation) and 60°C for 1 min (annealing extension). The primers and fluorogenic probes for PD-1, NKG2A, NKG2D, and glyceraldehyde-3-phosphate dehydrogenase (GAPDH) were obtained from the Taqman kit. The quantification of the gene expression was obtained using a sequence detector system software (Applied Biosystems).

Quantification of TILs. The cellular densities of $CD8^+$ T cells and $CD56^+$ NK cells in the tongue cancer and OLP were calculated manually using the immunohistochemical specimens as follows; 20 microscopic areas were independently selected at a high power magnification (×40 objective). One field corresponded to 0.071 mm^2. Positive cells in the cancer nests and those in the stroma were calculated separately. The number of groups compared was four; cancer nest, cancer stroma, OLP mucosa, and OLP submucosa. The number of positive cells in 20 areas in each specimen was averaged, and the results are expressed as the number of positive cells per square millimeter.

Morphometric analyses of $PD\text{-}1^+$, $NKG2D^+$, $NKG2A^+$, $CD69^+$, or $Ki\text{-}67^+$ cells among $CD8^+$ T cells and $CD56^+$ NK cells. We performed enzyme-linked double-labeling immunohistochemistry for these markers and CD8 or CD56 in all cases. We quantified the expression of each molecule in at least 20 independently selected areas containing abundant TILs (10 cancer nests and 10 cancer stroma) per one sample by the use of a ×40 objective. The following quantification was done using color photograph captured with an Olympus CCD camera. The positive rates were counted thrice manually from the photographs by the same observer (F.K.) with the supervision of another investigator (Y.W.). For the assessment of the double-positive cells, $CD8^+$ T cells or $CD56^+$ NK cells were counted first, followed by counts of the double-positive cells (each marker plus CD8 or CD56). The statistical analyses were performed with JSTAT software.[4] The Mann-Whitney *U* test was performed to compare the two groups when the Kruskal-Wallis test showed significant differences as a whole ($P < 0.05$). All analyses were repeated at least twice. The data are presented as box and whisker plots; the median value is shown within each box, the lower border represents the 25th percentile, and the upper border represents the 75th percentile. The whiskers show the 5th and 95th percentiles.

Results

Tissue distribution of immune cells in squamous cell carcinoma of the tongue: intraepithelial versus stromal. We analyzed 22 frozen specimens of the early-stage tongue cancer without any preoperative therapy. Based on observation of H&E staining, specimens containing cancer nests were thus selected and used in this study. We carefully discriminated between lymphocytes in the cancer nests (intraepithelial) and those in the cancer stroma (stromal). The cancer nest means a cluster of carcinoma cells, and the stroma means connective tissue areas around the cancer nests. The cancer nests were surrounded by abundant stromal lymphocytes in all specimens, especially richly along the tumor-host interface (Fig. 1*A*). The infiltrating cells in the stroma were mainly $CD4^+$ and $CD8^+$ T cells (Fig. 1*B* and *C*). In addition, $CD83^+$ and/or DC-Lamp$^+$ mature dendritic cells with a typical dendritic morphology were also observed (Fig. 2*A*). The stromal cells expressing CD56 were less frequent (Fig. 2*B*). The cancer nests were infiltrated by numerous intraepithelial $CD8^+$ T cells, very few $CD4^+$ cells, abundant $PD\text{-}1^+$ cells, and $CD56^+$ cells (Figs. 1*B–D* and 2*B*). The $CD56^+$ cells were judged to be NK cells because most of them expressed CD94, but not CD3, by double staining (not shown). Both $NKG2A^+$ and $NKG2D^+$ cells were present in the cancer nests at similar frequencies (Fig. 2*C* and *D*). In contrast, the cancer stroma was infiltrated only by $NKG2D^+$ cells (Fig. 2*D*) with $NKG2A^+$ cells being quite infrequent (not shown). The cancer nests were also infiltrated by $CD1a^+$/Langerin$^+$/$CD83^-$ immature dendritic cells (not shown). This was in sharp contrast to the abundant distribution of mature dendritic cells in the stroma (Fig. 2*A*). These data indicated the predominance of $PD\text{-}1^+$ cells and $NGK2A^+$ cells in the cancer nest.

Next, we quantitatively analyzed the numbers of TILs in the early-stage tongue cancer to compare those of OLP. The number of $CD8^+$ T cells in the cancer was similar to that of OLP (168 ± 98 cells/mm^2 in cancer nest versus 196 ± 70 cells/mm^2 in OLP mucosa; 686 ± 210 cells/mm^2 in cancer stroma versus 742 ± 336 cells/mm^2 in OLP submucosa). NK cells in the cancer nest (98 ± 58 cells/mm^2) far outnumbered those in the OLP mucosa (nearly absent, [0]). In contrast, the number of NK cells in the cancer stroma (67 ± 36 cells/mm^2) was roughly comparable with that of the OLP submucosa (101 ± 41 cells/mm^2).

Selective expression of PD-1, NKG2A, and NKG2D genes in clinically early-stage squamous cell carcinoma of the tongue. To confirm the expression of the corresponding mRNA in tissue, we performed quantitative real-time PCR. As shown in Fig. 3, PD-1 and NKG2A were expressed at much high levels in cancer tissues, whereas NKG2D was expressed at comparable levels in both cancer and lichen planus. No such strong expression of these genes was seen in normal tongue tissue specimens. However, the results obtained here were the sum of intraepithelial and stromal cells in the cancer and mucosal and submucosal cells in OLP and normal tissues, respectively.

Cellular identification of $PD\text{-}1^+$ and $NKG2A^+$ cells as intraepithelial $CD8^+$ T cells and NK cells, respectively. For the identification of $PD\text{-}1^+$ cells and $NKG2A^+$ cells, we performed a double immunofluorescent staining for six representative cases using fresh frozen specimens. As shown in Figs. 4 and 5*A*, most of $PD\text{-}1^+$ and $NKG2A^+$ cells in the cancer nests were double positive for CD8 and CD56, respectively. In contrast, the cancer stroma was only infrequently infiltrated by such double-positive cells ($PD\text{-}1^+CD8^+$ and $NKG2A^+CD56^+$; not shown).

Quantitative analyses of PD-1, NKG2A, NKG2D, CD69, and Ki-67 expression in squamous cell carcinoma compared with those in OLP. To clearly show the difference of activation status of TILs, we further compare the expression frequency of PD-1, NKG2A, NKG2D, CD69, and Ki-67 among $CD8^+$ and $CD56^+$ cells between tongue cancer and OLP, a positive control for the active

[4] Obtainable at vector.co.jp/soft/.

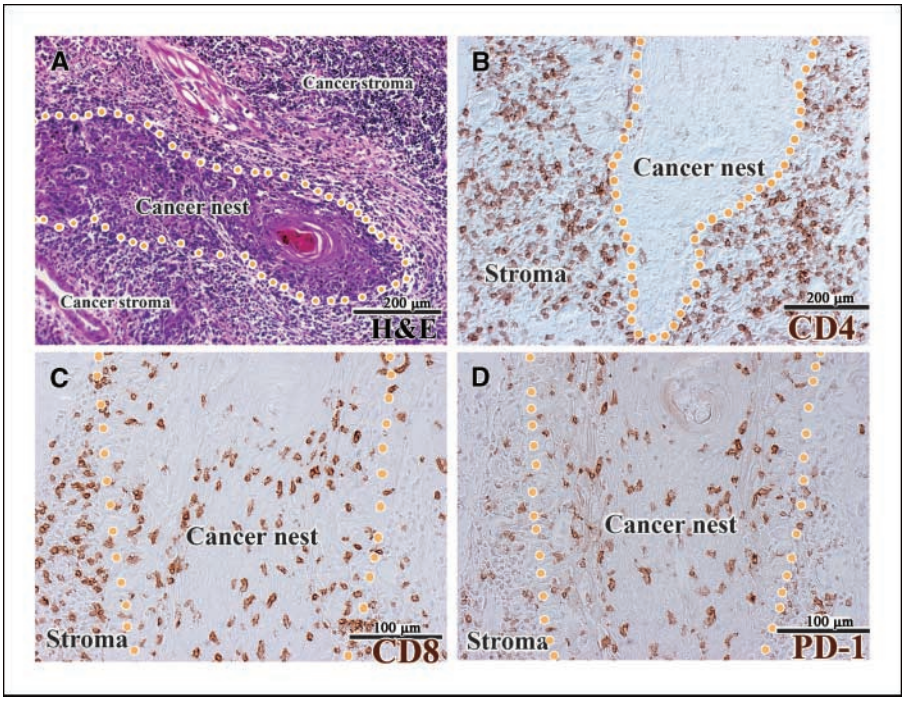

Figure 1. Representative pictures of squamous cell carcinoma of the tongue in the present study, all in a clinically early stage. Note the heavy lymphocytic infiltrate not only in the cancer stroma but also in the cancer nest (H&E staining; *A*). Immunohistochemistry for CD4 (*B*), CD8 (*C*), and PD-1 (*D*). Note that numerous $CD4^+$ T cells selectively infiltrate the cancer stroma, leaving the cancer nest free of $CD4^+$ T cells (virtually no intraepithelial $CD4^+$ T cells; *B*). Both $CD8^+$ and $PD\text{-}1^+$ cells infiltrated the cancer nest, as well as the cancer stroma (*C* and *D*). Note that the stromal $PD\text{-}1^+$ cells were apparently fewer than the stromal $CD8^+$ cells. *C* and *D,* serial frozen sections. *Yellow dots,* boundaries between the cancer nest and the cancer stoma.

CTL responses (summarized in Fig. 6). All these analyses were performed by enzyme-linked double immunohistochemistry in all cases using PLP-prefixed specimens as described in the Supplementary data. The intraepithelial $CD8^+$ T cells expressed PD-1 much more frequently than did those in the cancer stroma, the OLP mucosa, or the OLP submucosa (Fig. 6*A*). No significant differences were observed in the CD69 expression of $CD8^+$ T cells among these tissue groups (not shown). On the other hand, the intraepithelial $CD8^+$ T cells expressed NKG2D less frequently than did those in the cancer stroma and the OLP submucosa (Figs. 5*B* and 6*B*). We next performed an analysis on the proliferative activity of TILs using Ki-67, one of the representative proliferation-associated markers. The intraepithelial $CD8^+$ T cells were virtually negative for Ki-67 (Figs. 5*C* and 6*C*). In contrast, $CD8^+$ T cells in the cancer stroma frequently expressed Ki-67 (Figs. 5*D* and 6*C*) in a similar pattern to that of NKG2D (Figs. 5*B* and 6*B*). These results suggested that the intraepithelial $CD8^+$ T cells are mostly functionally suppressed, whereas the stromal $CD8^+$ T cells are in a more activated state as those in the OLP tissues. The intraepithelial $CD56^+$ cells expressed NKG2A at much higher

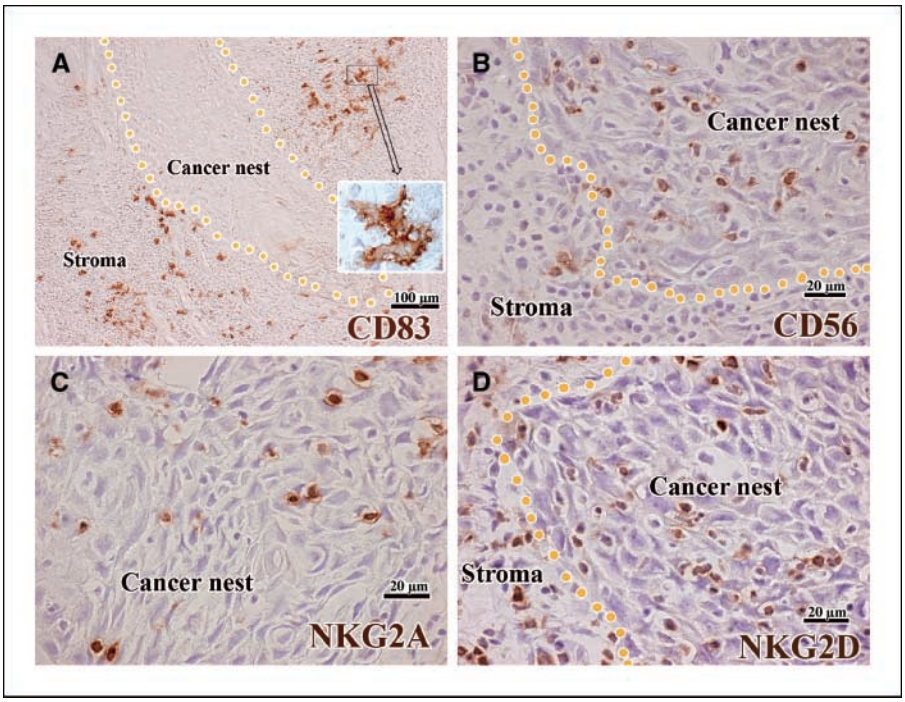

Figure 2. Immunohistochemistry for CD83, CD56, NKG2A,and NKG2D. *A,* infiltration of the cancer stroma by mature dendritic cells which show a typical dendritic morphology (*inset*). *B,* infiltration of the cancer nests by $CD56^+$ NK cells. *C,* infiltration of the cancer nest by $NKG2A^+$ cells. The immunoreactive cells for NKG2D infiltrated the cancer nest, as well as the cancer stroma (*D*). *Yellow dots,* boundaries between the cancer nest and the cancer stoma.

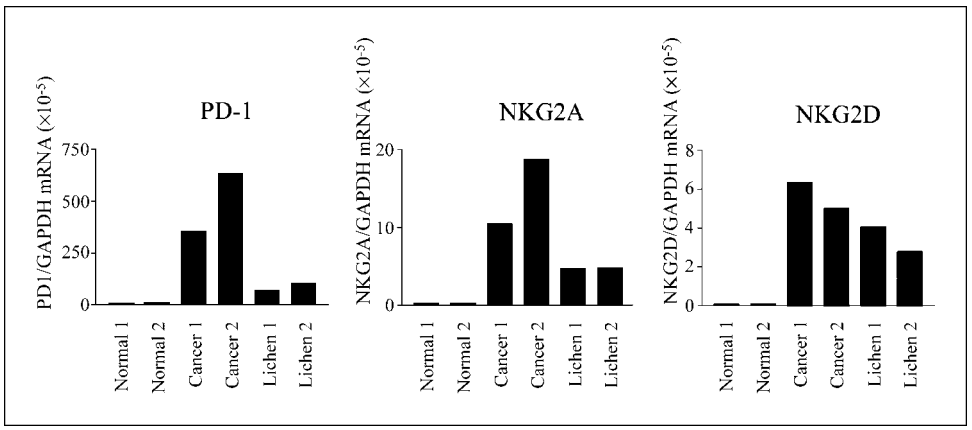

Figure 3. Quantitative real-time PCR analysis that confirms a higher tissue expression of mRNAs for PD-1, NKG2A, and NKG2D in tongue cancer than in OLP and normal mucosa. The results are expressed as the ratio to the expression of GAPDH housekeeping gene. *Columns,* representative results from two separate experiments.

frequencies than did those in the cancer stroma or in the OLP tissues (Fig. 6*D*), suggesting that the intraepithelial NK cells are also in a certain suppressed state. No significant differences were observed in the expression of NKG2D or CD69 on $CD56^+$ NK cells among these tissue groups (not shown). It is noteworthy that the activation status of $CD8^+$ T cells and NK cells in the stroma closely correlated with the selective distribution of mature dendritic cells in the cancer stroma (Fig. 2*A*).

We finally analyzed the correlation between the expression frequencies of PD-1 and NKG2A by $CD8^+$ T cells and NK cells, respectively, in the cancer tissues (n = 22). No statistically significant correlation was found between the two. This analysis also made it clearer that $CD8^+$ T cells and NK cells expressed PD-1 and NKG2A, respectively, at a far higher rate in the cancer nests than in the cancer stroma (Supplementary Fig. S1).

Discussion

Our present morphologic data using early-stage tongue squamous cell carcinomas have shown the immunophenotypical heterogeneity of the TILs in relation to their microanatomic locations: the relatively suppressed immunophenotypes of the intraepithelial TILs in contrast to the activated immunophenotypes of the stromal TILs. We also examined the immunophenotypes of the lymphocytes infiltrating the OLP for comparison. OLP is an autoimmune disease caused by a $CD8^+$ T cell–mediated immune attack against the basal epithelial cells in the oral mucosa (21). These comparative analyses confirmed that the activated phenotypes of stromal TILs are at a similar level to those in OLP. It is noteworthy that mature dendritic cells are distributed in both cancer stroma and OLP. Thus, the comparative analyses in the present study further strengthened the concept of the functional heterogeneity of the TILs in cancer, thus suggesting that the suppression of antitumor immunity could first take place in the cancer nests (22).

In head and neck cancer, Badoual et al. reported that the number of $CD4^+CD69^+$ T cells in the cancer stroma correlated with a better regional control, but they could not find any prognostic value of the stromal $CD8^+$ T cells (23). On the other hand, Naito et al. reported that $CD8^+$ TILs in the different microanatomic locations may have differing effects on the patients' prognosis in colorectal cancer,

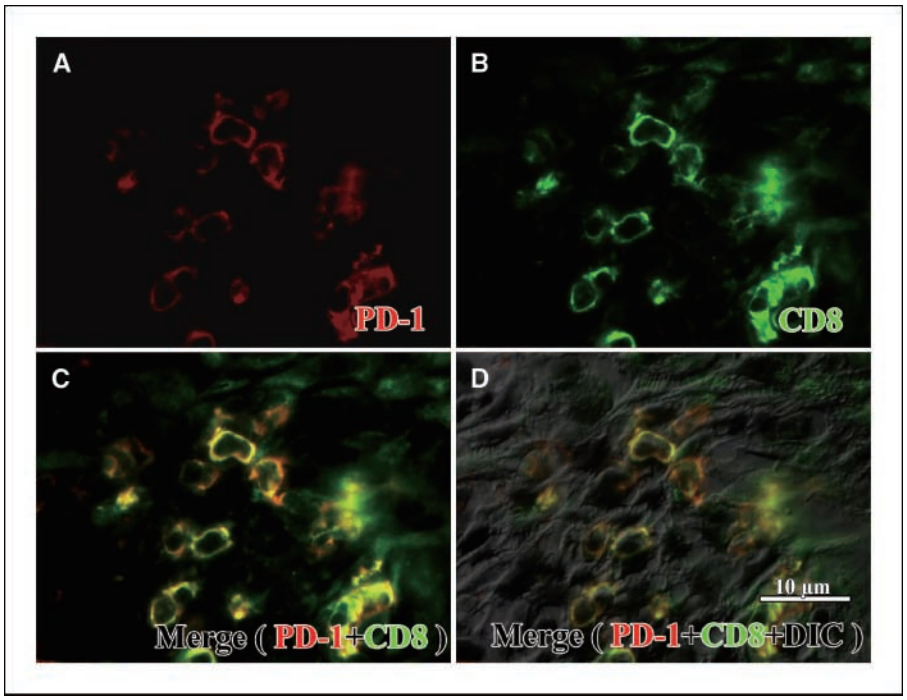

Figure 4. Double immunofluorescence staining for PD-1 and CD8 in the cancer nest. *Red,* PD-1 (*A*); *green,* CD8 (*B*); *yellow,* double-positive ($PD\text{-}1^+CD8^+$) cells (*C*). To show the presence of cancer cells, the double fluorescence image was further overlaid by the differential interference contrast (*DIC*) bright-field image (*D*).

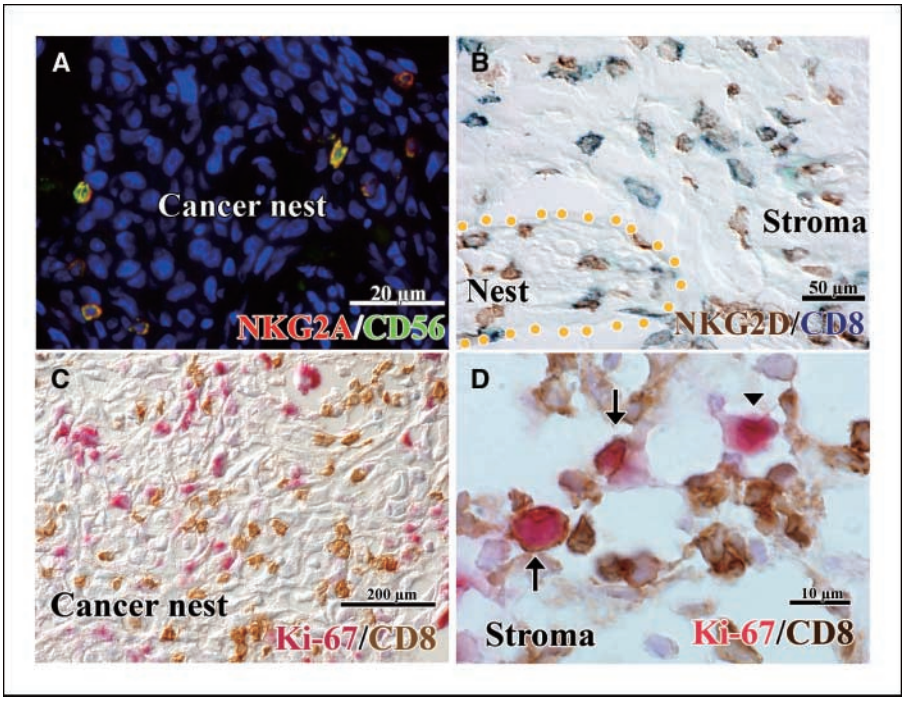

Figure 5. Double immunofluorescence labeling of NKG2A (*red*) and CD56 (*green*) in the cancer nest. Note double-positive (*yellow*; $NKG2A^+CD56^+$) cells in the cancer nest. The nuclei were counterstained by 4′,6-diamidino-2-phenylindole (*blue*; *A*). An enzyme-linked double immunostaining for the NKG2D (*brown*) and CD8 (*dark blue*) in the cancer nest and stroma of early-stage tongue cancer. Note numerous double-positive cells ($NKG2D^+CD8^+$) in the cancer stroma (*B*). Ki-67 expression on $CD8^+$ T cells in the cancer nest (*C*) and in the cancer stroma (*D*). Note the different distribution of $CD8^+$ T cells (*brown*) and Ki-67^+ cells (*red*) in the cancer nest (*C*), indicating that no $CD8^+$ T cells express Ki-67. In contrast, a certain subpopulation of $CD8^+$ T cells (*brown*) coexpress Ki-67 (*red*) in the cancer stroma (*D*). *Arrows,* double-positive cells for Ki-67 and CD8 (*D*); *arrowhead,* single positive cell for Ki-67 (*D*).

with the intraepithelial $CD8^+$ T cells being the most important (2). These led us to analyze the immunophenotypical status of the TILs in different microanatomic localizations in early-stage tongue cancer tissue specimens.

The present study has shown that the intraepithelial $CD8^+$ TILs express PD-1 at a high rate and NKG2D at a low rate. In contrast, the stromal $CD8^+$ TILs, as well as $CD8^+$ T cells in the OLP, express PD-1 at low rates. The high expression rate of PD-1 by the intraepithelial $CD8^+$ TILs suggests their exhausted functions (10). It has been already documented that oral squamous cell carcinoma expresses PD-L1 (24), and we also have observed that PD-1^+ TILs coexist with PD-$L1^+$ tumor cells in the cancer nests of early-stage tongue cancer.[5] This *in vivo* close contact suggests one of the immune evasion mechanisms by the cancer cells (25, 26). In contrast, mucosal $CD8^+$ T cells in OLP expressed PD-1 at a far lower rate, thus suggesting that OLP mucosal $CD8^+$ T cell may survive and continue to exert their function (9). This may explain the reason of sustained damages to the epithelial cells in OLP.

In accordance with the high expression of PD-1, the intraepithelial $CD8^+$ TILs show a much lower expression of NKG2D than do the stromal $CD8^+$ TILs. NKG2D is one of the most potent activating receptors for the effector functions of both $CD8^+$ T cells and NK cells in peripheral tissues (15, 16, 27–29). Our data, thus far, indicate that the intraepithelial $CD8^+$ T cells are phenotypically inactivated. Indeed, at early stage of tumor development, NKG2D can effectively reject the tumor cells (15). However, sustained surface expression and proteolytic shedding of MICA, a NKG2D ligand, by tumor cells impair the immune response, thus promoting tumor immune evasion (27–29). The intraepithelial $CD8^+$ TILs express Ki-67 only at a very low rate, whereas both the stromal $CD8^+$ TILs and the submucosal $CD8^+$ T cells in OLP show high rates of expression of Ki-67. The increased proliferative activity of the stromal $CD8^+$ T cells is probably related to the abundant distribution of mature dendritic cells in the cancer stroma and the submucosa of OLP, thus suggesting the presence of a certain level of ongoing immune responses. The loss of the proliferative activity in the intraepithelial $CD8^+$ T cells is also consistent with their high rates of expression of PD-1.

Our results are in contrast to the highly suppressed state of the lymphocytes, both in the circulating blood and in the cancer stroma of oral cancer patients with the advanced stages (mostly stage III or stage IV; ref. 30). This discrepancy may be ascribed to the different stages of disease. The previous analyses of the immune cells in colorectal cancer may support this notion. The number of intraepithelial $CD8^+$ T cells negatively correlates with the cancer stages; they are the highest in stage I and show decreases in the advanced stages (31).

We also analyzed the functional phenotypes of NK cell, another possible effector cell. NKG2A was more prominently expressed on the intraepithelial NK cells than those in the cancer stroma or in the OLP, suggesting the suppressed function of the intraepithelial NK cells, quite similar to the high PD-1 expression on the intraepithelial $CD8^+$ T cells (13, 32). Therefore, the intraepithelial NK cells might have partially lost a tumor-specific triggering capacity (8).

Taken together, the intraepithelial $CD8^+$ TILs, as well as the intraepithelial NK cells, in our clinically early-stage tongue cancer are in a certain state of an inactivated phenotype and are poor in the proliferation activity in sharp contrast to the more activated phenotype of their stromal counterparts. Given the systemically immunosuppressed status in patients with an advanced stage cancer, we have possibly visualized in humans the ongoing immune evasion process that initially starts in the cancer nest (33–35).

Finally, we need to pay attention to the possible differences among various cancers. For example, the intraepithelial $CD8^+$ T cells in a colorectal cancer express Ki-67 at levels higher than do the stromal $CD8^+$ T cells (31). In renal cell carcinoma, a higher labeling index of Ki-67 in the intraepithelial $CD8^+$ T cells

[5] F. Katou, H. Ohtani, Y. Watanabe, unpublished data.

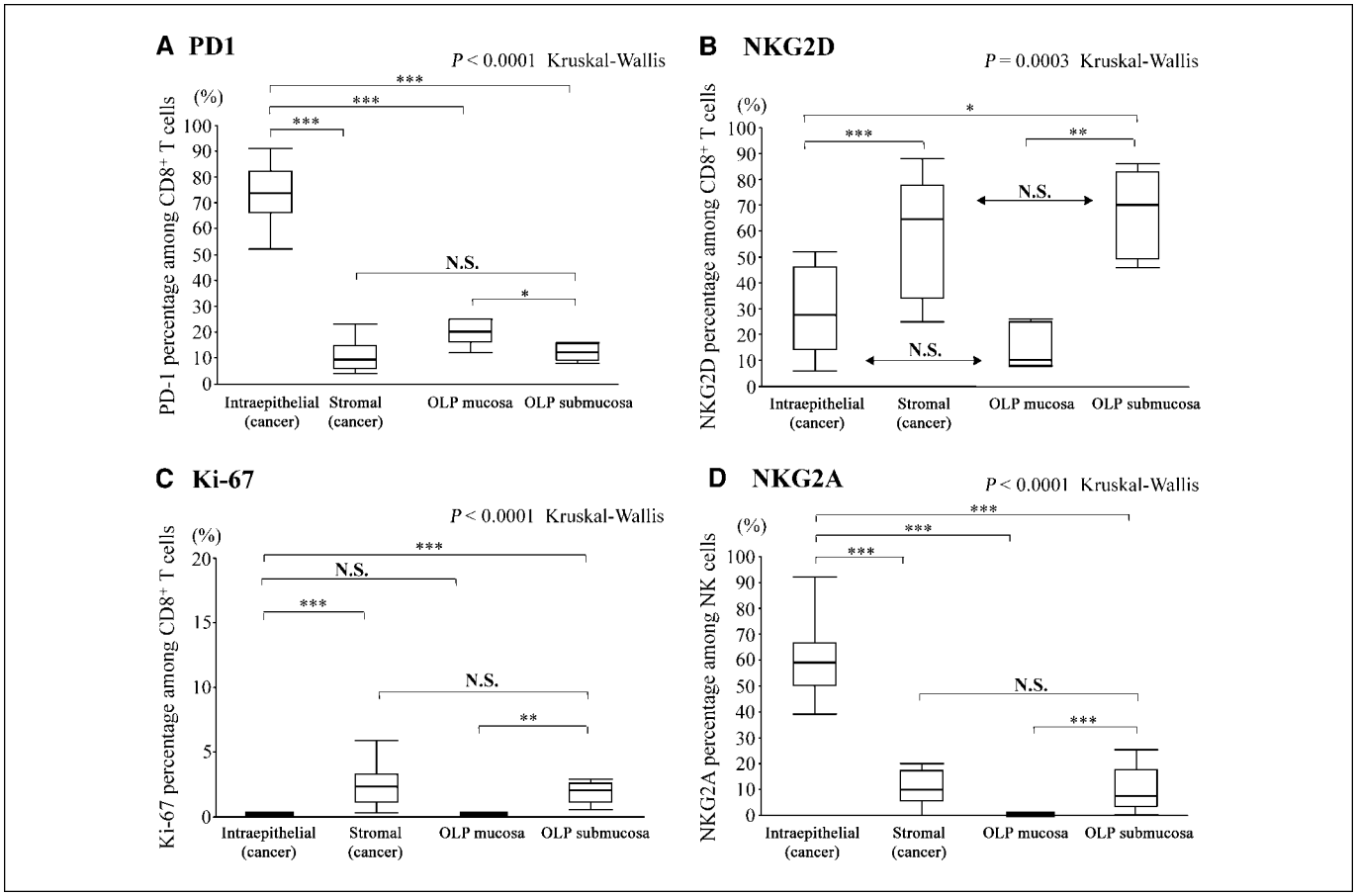

Figure 6. Expression frequencies of PD-1, NKG2D, Ki-67, and NKG2A among $CD8^+$ T cells or $CD56^+$ NK cells in early-stage tongue cancer and OLP, as measured by an enzyme-linked double immunostaining (Fig. 4*B–D*). The data were derived from all cases examined. Note that the intraepithelial $CD8^+$ T cells express PD-1 most frequently (*A*) and NKG2D at a relative low rate (*B*), and they are virtually negative for Ki-67 (*C*). The stromal $CD8^+$ T cells express NKG2D and Ki-67 at a similar rate to those in the OLP submucosa (*B* and *C*). Expression frequencies of NKG2A among the $CD56^+$ NK cells in early-stage tongue cancer and OLP (*D*). Note that the intraepithelial NK cells express NKG2A most frequently. The data are presented as the median ± 75% quartiles in box plots due to their nonparametric distribution. The whiskers show the 5th and 95th percentiles. Statistical significance was evaluated by the Kruskal-Wallis test followed by the Mann-Whitney *U* test between two particular groups. *, $P < 0.05$; **, $P < 0.01$; ***, $P < 0.001$.

significantly correlates to a longer survival of patients (36). These are adenocarcinomas. Our present data are based on squamous cell carcinoma of the tongue. Therefore, it must be kept in mind that the immune responses could vary with the different histologic types of cancer.

To conclude, we herein showed the importance of the analyses of the TIL properties in relation to their *in situ* localization. The further accumulation of knowledge on the TILs in different stages of various human cancers may help to develop a more effective design for immunostimulatory therapy.

Acknowledgments

Received 7/26/2007; revised 9/27/2007; accepted 10/3/2007.

The costs of publication of this article were defrayed in part by the payment of page charges. This article must therefore be hereby marked *advertisement* in accordance with 18 U.S.C. Section 1734 solely to indicate this fact.

References

1. Zitvogel L, Tesniere A, Kroemer G. Cancer despite immunosurveillance: immunoselection and immunosubversion. Nat Rev Immunol 2006;6:715–27.
2. Naito Y, Saito K, Shiiba K, et al. $CD8^+$ T cells infiltrated within cancer cell nests as a prognostic factor in human colorectal cancer. Cancer Res 1998;58:3491–4.
3. Sato E, Olson SH, Ahn J, et al. Intraepithelial $CD8^+$ tumor-infiltrating lymphocytes and a high $CD8^+$/regulatory T cell ratio are associated with favorable prognosis in ovarian cancer. Proc Natl Acad Sci U S A 2005; 102:18538–43.
4. Galon J, Costes A, Sanchez-Cabo F, et al. Type, density, and location of immune cells within human colorectal tumors predict clinical outcome. Science 2006; 313:1960–4.
5. Boissonnas A, Fetler L, Zeelenberg IS, Hugues S, Amigorena S. *In vivo* imaging of cytotoxic T cell infiltration and elimination of a solid tumor. J Exp Med 2007;204:345–56.
6. Moretta A, Poggi A, Pende D, et al. CD69-mediated pathway of lymphocyte activation: anti-CD69 monoclonal antibodies trigger the cytolytic activity of different lymphoid effector cells with the exception of cytolytic T lymphocytes expressing T cell receptor α/β. J Exp Med 1991;174:1393–8.
7. Lopez-Cabrera M, Santis AG, Fernandez-Ruiz E, et al. Molecular cloning, expression, and chromosomal localization of the human earliest lymphocyte activation antigen AIM/CD69, a new member of the C-type animal lectin superfamily of signal-transmitting receptors. J Exp Med 1993;178:537–47.
8. North J, Bakhsh I, Marden C, et al. Tumor-primed human natural killer cells lyse NK-resistant tumor targets: evidence of a two-stage process in resting NK cell activation. J Immunol 2007;178:85–94.
9. Freeman GJ, Long AJ, Iwai Y, et al. Engagement of the PD-1 immunoinhibitory receptor by a novel B7 family member leads to negative regulation of lymphocyte activation. J Exp Med 2000;192:1027–34.
10. Barber DL, Wherry EJ, Masopust D, et al. Restoring function in exhausted CD8 T cells during chronic viral infection. Nature 2006;439:682–7.
11. Cerwenka A, Lanier LL. Natural killer cells, viruses and cancer. Nat Rev Immunol 2001;1:41–9.

12. Zhang C, Zhang J, Wei H, Tian Z. Imbalance of NKG2D and its inhibitory counterparts: how does tumor escape from innate immunity? Int Immunopharmacol 2005;5:1099–111.

13. Brooks AG, Posch PE, Scorzelli CJ, Borrego F, Coligan JE. NKG2A complexed with CD94 defines a novel inhibitory natural killer cell receptor. J Exp Med 1997; 185:795–800.

14. Masilamani M, Nguyen C, Kabat J, Borrego F, Coligan JE. CD94/NKG2A inhibits NK cell activation by disrupting the actin network at the immunological synapse. J Immunol 2006;177:3590–6.

15. Bauer S, Groh V, Wu J, et al. Activation of NK cells and T cells by NKG2D, a receptor for stress-inducible MICA. Science 1999;285:727–9.

16. Smyth MJ, Swann J, Cretney E, et al. NKG2D function protects the host from tumor initiation. J Exp Med 2005; 202:583–8.

17. Sugerman PB, Savage NW, Walsh LJ, et al. The pathogenesis of oral lichen planus. Crit Rev Oral Biol Med 2002;13:350–65.

18. Iijima W, Ohtani H, Nakayama T, et al. Infiltrating $CD8^+$ T cells in oral lichen planus predominantly express CCR5 and CXCR3 and carry respective chemokine ligands RANTES/CCL5 and IP-10/CXCL10 in their cytolytic granules: a potential self-recruiting mechanism. Am J Pathol 2003;163:261–8.

19. Katou F, Ohtani H, Nakayama T, et al. Macrophage-derived chemokine (MDC/CCL22) and CCR4 are involved in the formation of T lymphocyte-dendritic cell clusters in human inflamed skin and secondary lymphoid tissue. Am J Pathol 2001;158:1263–70.

20. Katou F, Ohtani H, Nakayama T, Nagura H, Yoshie O, Motegi K. Differential expression of CCL19 by $DC\text{-}Lamp^+$ mature dendritic cells in human lymph node versus chronically inflamed skin. J Pathol 2003;199:98–106.

21. Santoro A, Majorana A, Bardellini E, et al. Cytotoxic molecule expression and epithelial cell apoptosis in oral and cutaneous lichen planus. Am J Clin Pathol 2004;121: 758–64.

22. Pardoll D. Does the immune system see tumors as foreign or self? Annu Rev Immunol 2003;21:807–39.

23. Badoual C, Hans S, Rodriguez J, et al. Prognostic value of tumor-infiltrating $CD4^+$ T-cell subpopulations in head and neck cancers. Clin Cancer Res 2006;12:465–72.

24. Tsushima F, Tanaka K, Otsuki N, et al. Predominant expression of B7-1 and its immunoregulatory roles in oral squamous cell carcinoma. Oral Oncol 2006;42: 268–74.

25. Iwai Y, Ishida M, Tanaka Y, Okazaki T, Honjo T, Minato N. Involvement of PD-L1 on tumor cells in the escape from host immune system and tumor immunotherapy by PD-L1 blockade. Proc Natl Acad Sci U S A 2002;99:12293–7.

26. Dong H, Strome SE, Salomao DR, et al. Tumor-associated B7-1 promotes T-cell apoptosis: a potential mechanism of immune evasion. Nat Med 2002;8:793–800.

27. Groh V, Wu J, Yee C, Spies T. Tumour-derived soluble MIC ligands impair expression of NKG2D and T-cell activation. Nature 2002;419:734–8.

28. Jamieson AM, Diefenbach A, McMahon CW, Xiong N, Carlyle JR, Raulet DH. The role of the NKG2D immunoreceptor in immune cell activation and natural killing. Immunity 2002;17:19–29.

29. Groh V, Smythe K, Dai Z, Spies T. Fas-ligand-mediated paracrine T cell regulation by the receptor NKG2D in tumor immunity. Nat Immunol 2006;7: 755–62.

30. Reichert TE, Strauss L, Wagner EM, Gooding W, Whiteside TL. Signaling abnormalities, apoptosis, and reduced proliferation of circulating and tumor-infiltrating lymphocytes in patients with oral carcinoma. Clin Cancer Res 2002;8:3137–45.

31. Chiba T, Ohtani H, Mizoi T, et al. Intraepithelial $CD8^+$ T-cell-count becomes a prognostic factor after a longer follow-up period in human colorectal carcinoma: possible association with suppression of micrometastasis. Br J Cancer 2004;91:1711–7.

32. Speiser DE, Pittet MJ, Valmori D, et al. *In vivo* expression of natural killer cell inhibitory receptors by human melanoma-specific cytolytic T lymphocytes. J Exp Med 1999;190:775–82.

33. Zhang L, Conejo-Garcia JR, Katsaros D, et al. Intratumoral T cells, recurrence, and survival in epithelial ovarian cancer. N Engl J Med 2003;348:203–13.

34. Dunn GP, Old LJ, Schreiber RD. The immunobiology of cancer immunosurveillance and immunoediting. Immunity 2004;21:137–48.

35. Jewett A, Head C, Cacalano NA. Emerging mechanisms of immunosuppression in oral cancers. J Dent Res 2006;85:1061–73.

36. Nakano O, Sato M, Naito Y, et al. Proliferative activity of intratumoral $CD8^+$ T-lymphocytes as a prognostic factor in human renal cell carcinoma: clinicopathologic demonstration of antitumor immunity. Cancer Res 2001; 61:5132–6.

Differing Phenotypes between Intraepithelial and Stromal Lymphocytes in Early-Stage Tongue Cancer

Fuminori Katou, Haruo Ohtani, Yoshiko Watanabe, et al.

Cancer Res 2007;67:11195-11201.